Energy and Buildings 126 (2016) 2–13

Contents lists available at ScienceDirect

Energy and Buildings

journal homepage: www.elsevier.com/locate/enbuild

Simulation and optimization study on a solar space heating system combined with a low temperature ASHP for single family rural residential houses in Beijing

Jie Deng[a,b,*], Zhiyong Tian[b], Jianhua Fan[b], Ming Yang[a], Simon Furbo[b], Zhifeng Wang[a]

[a] Key Laboratory of Solar Thermal Energy and Photovoltaic System, Institute of Electrical Engineering, Chinese Academy of Sciences, Beijing 100190, PR China

[b] Department of Civil Engineering, Technical University of Denmark, Brovej 118, Kgs. Lyngby, DK 2800, Denmark

ARTICLE INFO

Article history:
Received 26 March 2016
Received in revised form 6 May 2016
Accepted 7 May 2016
Available online 11 May 2016

Keywords:
Solar space heating for single family houses
Air source heat pump (ASHP)
System parameter optimization
Economic analysis

ABSTRACT

A pilot project of the solar water heating system combined with a low temperature air source heat pump (ASHP) unit was established in 2014 in a detached residential house in the rural region of Beijing, in order to investigate the system application prospect for single family houses via system optimization design and economic analysis. The established system was comprised of the glass heat-pipe based evacuated tube solar collectors with a gross area of 18.8 m^2 and an ASHP with a stated heating power of 8 kW for the space heating of a single family rural house of 81.4 m^2. The dynamic thermal performance of the pilot system was measured for continuous 20 days under typical cold climate conditions and the test data was used to validate the TRNSYS simulation model established. On the basis of model validation, system optimizations of both the existing pilot household and the typical rural house with good building insulation were undertaken to figure out the system economical efficiency in the rural regions of Beijing. The results show that the payback periods of the solar space heating system combined with the ASHP with the collector areas 15.04–22.56 m^2 are 17.3–22.4 years for the established pilot household on the current electricity price level of 0.5 RMB/kWh, comparing with the reference condition of the fully ASHP space heating. It is further found that the equivalent solar heat price per kWh is too high under the current solar market cost price and collector technology. To put forward the integrated solar space heating for reducing carbon emission, it is suggested that the Beijing municipal government should offer some financial subsidy to compensate the equivalent solar heat price per kWh.

1. Introduction

Rural buildings in China account for more than half of the total building energy consumptions of the country in recent years [1]. It is reported that the use of coal and biomass for space heating and cooking may contribute 15–20% of primary $PM_{2.5}$ emissions in Beijing [2]. It is therefore an urgent demand to develop building energy conservation and renewable energy utilization for carbon emission reduction in the rural regions of China as the increase of frequently appeared haze days contributing to the environment deterioration. Although the government has been advocating the retrofit of existing residential buildings for energy conservation since 2005 via plenty of policy supporting projects, there is still a huge potential to push forward energy savings and renewable energy in the rural residential houses due to many obstacles [3].

Solar space heating combined with some auxiliary sources such as the air-source heat pump, biomass boiler is one of the promising ways of developing renewable energy and energy saving in the rural region of northern China. Shan et al. [4] studied the thermal performance of a combined solar heating system integrated with the ASHP in a simulated rural house. They measured the energy supply of the system for space heating in two different running modes under typical cold climate conditions of Beijing. And they successfully reduced 25% electricity consumption of the ASHP by reasonably adjusting the running procedures of the system. However, the economical payback period of the solar space heating system was not considered. The economical efficiency of the solar space heating combined with ASHP, which is a key factor in promoting the system application in rural regions of northern China, should be pay more attention on. Li et al. [5] studied an active solar

* Corresponding author at: Institute of Electrical Engineering (IEE), Chinese Academy of Sciences (CAS), No. 6, Beier Alley, Zhongguancun, Haidian District, Beijing 100190, PR China.
E-mail address: deng-jie2@163.com (J. Deng).

http://dx.doi.org/10.1016/j.enbuild.2016.05.019
0378-7788/

water heating system coupled with coal-fired boiler for the space heating of a new rural residence with 60 mm extruded polystyrene in Gansu province, China. They argued that the active solar heating system and the external wall insulation increased 14.5% of the initial cost of the new rural residence, with an energy saving fraction of 78% and a payback period of about 4.4 years compared to the reference residence of coal-fired heating without insulation. But it is puzzled that they did not mention the solar fraction/contribution ratio of the coupled heating system. Arsalis and Alexandrou [6] conducted the parametric study and cost analysis of a solar heating and cooling (SHC) system for the detached single-family households in hot climates. The cost analysis of the SHC system made by them was on the basis of cost assumptions of the system components and auxiliary energy, rather than real engineering costs. It was concluded that the SHC system would be unfavorable to compete with electric heat pump technology if the unit solar collector cost is above $ 360/m^2. Huang et al. [7] evaluated the solar water heating systems for United State typical residential buildings from the energetic, economic and environmental perspectives. The results showed that the energetic and environmental payback periods for solar water heating systems are less than half a year, and the life cycle cost payback for the systems vary from 4 to 13 years for different cities and different configurations when using the conventional electrical water heating systems in each city as the benchmark. Besides, the assessment method of the life cycle cost was widely used for energy supply systems [8] to obtain the payback period. It was argued by Li et al. [9] that the usage of renewable energy sources was constrained by high initial costs and long-term payback for building space heating. They presented an empirical research work to improve the design of the control system and the performance of an integrated heating system utilizing renewable energy sources by means of a geothermal field, solar energy, and drain water heat recovery system.

As a matter of fact, solar space heating for buildings especially for the detached single family households is not widely promoted in northern china due to many factors, such as building energy saving retrofit, the design levels of the solar heating system and system control strategy, economical efficiency, etc. In the present study, a pilot project of a solar heating system combined with an ASHP unit was established in a detached residential house in the rural region of Beijing, in order to investigate the system application prospect via system optimization design and economic analysis. Parameter optimization and running control strategy of the system were analyzed. And the life cycle cost of the solar system was assessed on the benchmark of totally ASHP space heating considering the investment and operating costs of the system in real pilot engineering.

Fig. 1. The pilot household of the solar space heating system combined with a ASHP in the rural region of Beijing.

The payback period of the solar space heating system combined with the ASHP unit was discussed for a typical single family rural house based on the system optimization and building insulation.

2. The established pilot project and field test

2.1. Pilot project of a solar heating system combined with a ASHP unit for a rural residential house

A pilot project of the solar water heating system combined with a low temperature ASHP unit was established in 2014 in a typical detached residential house in the surrounding rural region of Beijing (40°27′10″N; 115°52′17″E) for space heating. Fig. 1 shows the extrinsic feature of the pilot household. Fig. 2 gives the plane layout and size of the pilot household, which is composed of 6 rooms with a total building area of 122 m^2, while only Rooms 1–4 need space heating in reality. Thus the building space heating area is 81.4 m^2 (14.8 m by 5.5 m).The house exterior wall adopts 370 mm common brick masonry with 60 mm thickness EPS (expanded polystyrene) insulation, except for the south wall without thermal insulation layer. Thickness of the interior wall (also built by common brick) is 150 mm. Both the windows and the doors adopt double-layer plastic steel material. The eaves height of the house is 2.7 m and the summit height of the pitched roof is 4.3 m. Each window height is 1.6 m and the door height is 2.4 m.

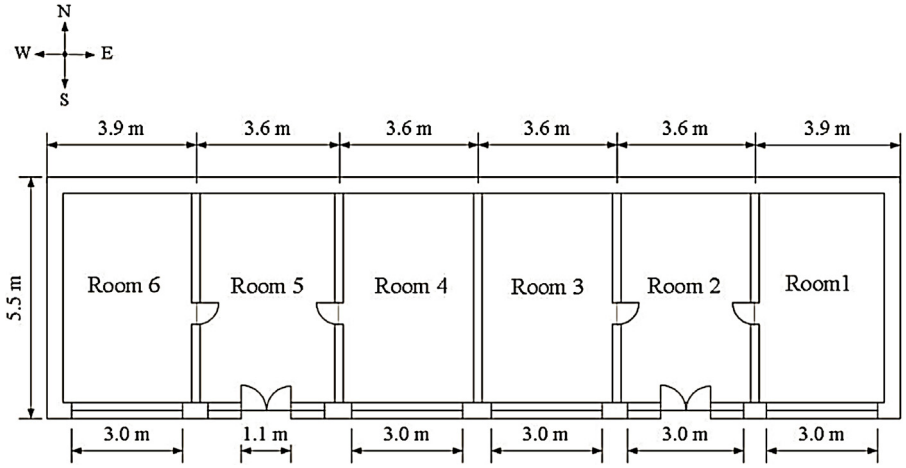

Fig. 2. Plane layout and size of the rural pilot household.

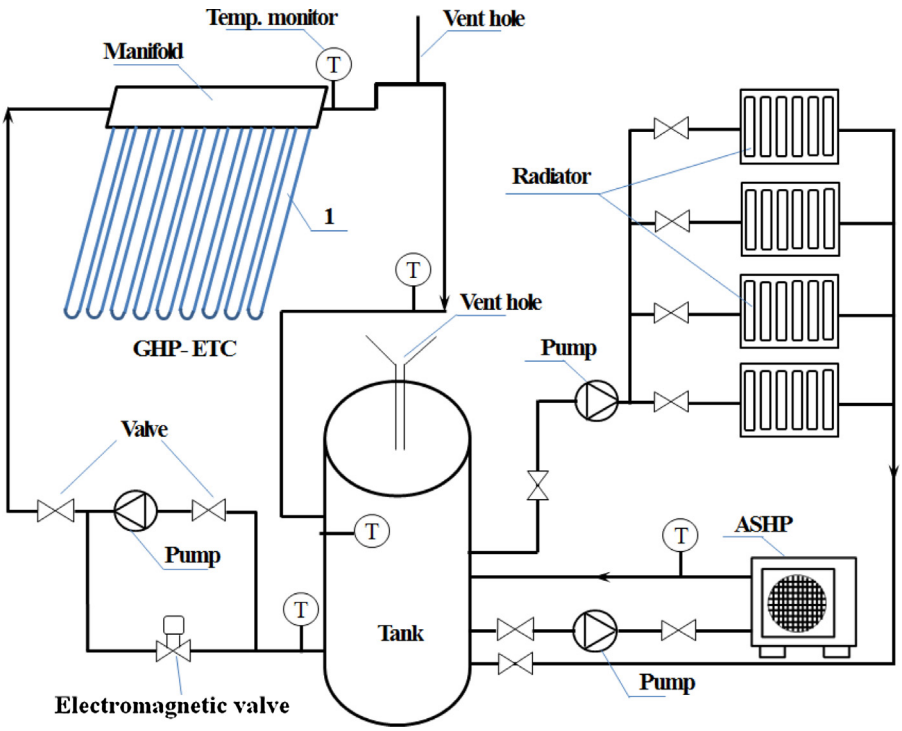

Fig. 3. Schematic diagram of the integrated space heating system.

The solar heating system is comprised of 5 glass heat-pipe based evacuated tube solar collector (GHP-ETC) modules with a total collector gross area of 18.8 m^2 (3.76 m^2 in gross area and 2.56 m^2 in aperture area for each collector module), a short-term thermal storage tank of 300 L, a circulating pump and a circulating start/stop controller using temperature difference between the solar heating system outlet temperature and the tank bottom temperature. Installation angle of the collector is 45°. It is an open-type system and the working fluid is water. To anti-freeze an automatic emptying strategy is designed in the controller to discharge the water out of the solar collector pipes after sunset or in cloudy sky and to draw water from the tank to the pipes for heat collection when good solar irradiance appears. The horizontal pipes are installed with a slope gradient of 0.005. Water in the solar system pipeline is emptied by gravitational force through an electromagnetic valve when the water return temperature is lower than a setting value (default 35 °C). In addition, a low-temperature enhanced vapor injection ASHP unit with the lowest operating temperature of −20 °C is used to supply heat when solar energy is insufficient. The stated heating power of the ASHP is 8 kW and the stated input electrical power is 2.25 kW. The start and stop of the ASHP are controlled by an automatic controller through the monitoring temperature of the water storage tank. The schematic operating of the integrated space heating system is shown in Fig. 3.

The logical running control of the sub-systems is sketched in Fig. 4. As shown in Fig. 4 (a), the start and stop of the pump in the solar collecting circulation is implemented by temperature difference control between the collector outlet and the tank bottom temperatures. The default start and stop temperature differences are 7 °C and 1 °C, respectively. The temperature difference can be changed. The start and stop conditions of the ASHP and the heat supply are managed by controlling the target temperatures of the tank and Room 1 to be 45 ± 5 °C and 18 ± 1 °C, respectively, as seen in Fig. 4 (b) and (c). The default target temperatures of the tank and Room 1 are 45 °C, 18 °C, respectively, which can be manually chosen.

2.2. Dynamic thermal performance tests of the space heating system for the pilot household

For the field test of the system thermal performance, the inlet and outlet temperatures, the volume flow rates, the accumulated heat quantities of the solar system, the ASHP unit and the main pipes of heat supply were recorded using data logger. The global solar irradiance on the inclined collector surface and the horizontal surface, ambient temperature, indoor temperature of Room 1 (see Fig. 2) were also monitored. Time interval of the data acquisition was 5 min. The measuring instruments and corresponding accuracies are listed in Table 1.

The energy balance of the water storage tank is described by Eq. (1).

$$\Delta Q_{tank} = Q_{solar} + Q_{ASHP} - Q_{supply} - Q_{tank,loss} \quad (1)$$

where ΔQ_{tank} denotes the internal energy change of the tank during a period, MWh; Q_{solar} represents the heat collected by the solar system, MWh; Q_{ASHP} stands for the heat supplied by the ASHP unit, MWh; Q_{supply} indicates the heat supply to the heating terminals (radiators), MWh; $Q_{tank,loss}$ means the heat loss to the room where the tank is located through tank and pipe surfaces.

The solar fraction f is calculated by:

$$f = \frac{Q_{solar}}{Q_{solar} + Q_{ASHP}} \quad (2)$$

The average thermal efficiency η_{coll} of the solar collecting system is obtained by:

$$\eta_{coll} = \frac{3.6 \times 10^9 \times Q_{solar}}{\int_0^\tau G_{global} \times A_{gross} d\tau} \quad (3)$$

where G_{global} represents the global solar irradiance incident on the collector tilted surface, W/m^2; A_{gross} is the total collector gross areas of the solar heating system, m^2; the multiplier 3.6×10^9 before Q_{solar} (the heat collected by the solar heating system) considers the unit conversion of MWh to J.

The average coefficient of performance (COP) of the ASHP can be gotten with the electricity consumption E_{ASHP} measured by the electricity meter during test period.

$$COP = \frac{Q_{ASHP}}{E_{ASHP}} \quad (4)$$

Dynamic thermal performance field tests of continuous 20 days were conduct from Jan. 1st, to Jan. 20th, 2016. Fig. 5 shows the test meteorological conditions and monitored indoor temperature of Room 1. The average outdoor temperature was −7.7 °C under the typical cold climate conditions. The volume flow rate of the solar system, the ASHP unit and the main pipes of heat supply were 0.6, 0.9, 0.8 m^3/h, respectively. During the 20 days test period, the total accumulated heat supply was 2.82 MWh, 0.59 MWh out of which was contributed by the solar collecting system. It meant that the solar fraction of the integrated system was 20.9% for space heating. According to the total accumulated heat supply 2.82 MWh and continuously 24 h heat supply for 81.4 m^2 rooms, the average heat supply power was 5.6 kW and the average measured heat load index was 68.7 W/m^2. The average COP of the ASHP during the period was 1.84.

3. TRNSYS based system simulation model and model validation

To optimize the system parameters and design based on TRNSYS 17.2 [10] it is firstly needed to establish the TRNSYS based system simulation model and execute the model validation with the field test results.

3.1. Thermal performance simulation model of the space heating system

According to the structural size of the pilot household (see Fig. 2), the geometrical 3-dimentional multi-zone building model was built using Google SketchUp 8.0 embedded with Trnsys 3d plug-in tool, as shown in Fig. 6. Thermophysical property parameters of the building envelope surfaces of the rural house were set as per the detailed building structures listed in Table 2. Table 3 gives the calculated comprehensive heat transfer coefficients (U-values) of the building envelopes.

The TRNSYS based simulation model for the integrated space heating system is shown in Fig. 7. Because there was not heat demand for Rooms 5 and 6 during the test, only Rooms 1 – 4 were connected to terminal radiators. The main TRNSYS components and parameters adopted were explained in Table 4.

3.2. Model validation

Meteorological conditions of January 1st to 20th, 2016 were used as the input meteorological conditions for the model validation. And 7 days' meteorological conditions (each day the same as January 1st) were added to the input data in order to remove the initial thermal inertia of the building since the studied rural house started space heating 1.5 months ago. The target temperature of the tank and the Room 1 were controlled to be 45 ± 5 °C, 18 ± 1 °C, respectively, according to the field test conditions. The simulated time step was 5 min which was the same as the test data. The total simulation time was 648 h, 168 h (24 h by 7) out of which took into accounted the initial thermal inertia. Fig. 8 gives the simulated temperatures of Rooms 1–6 during the 20 days test period

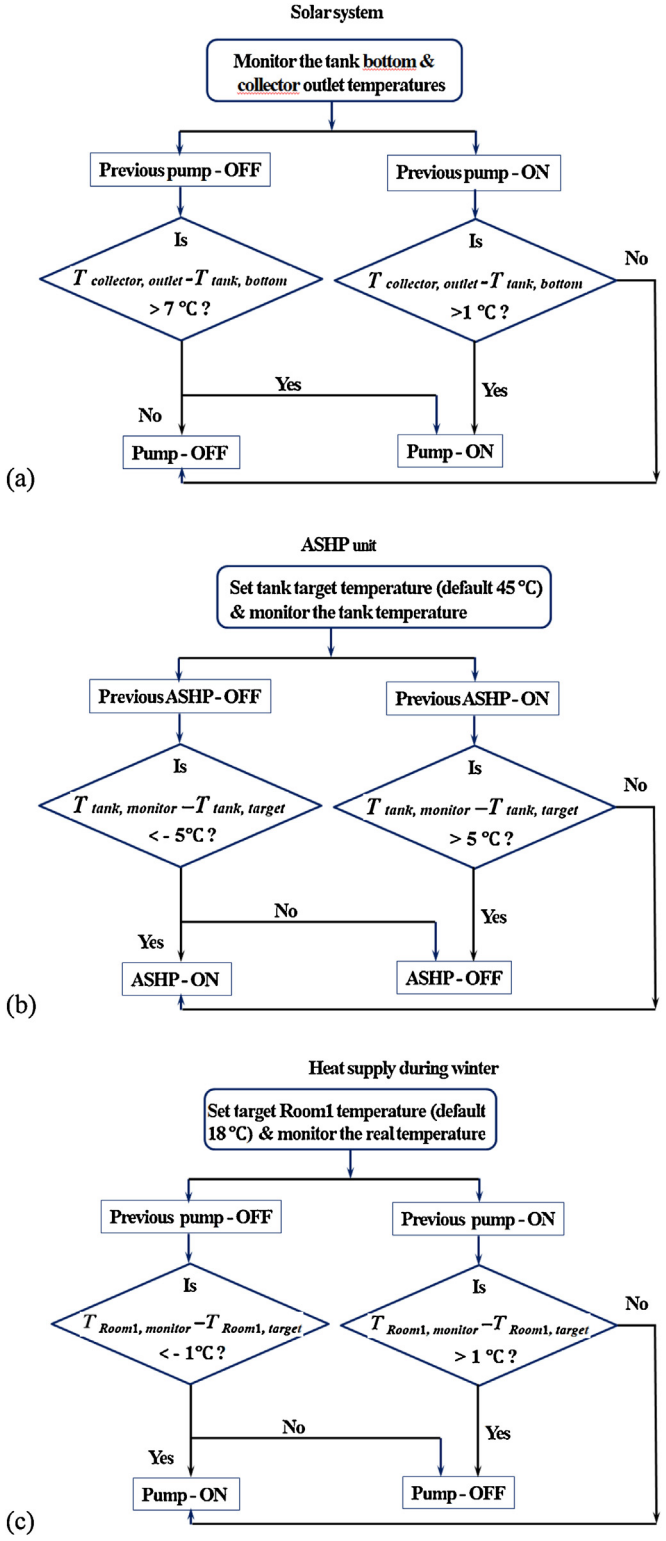

Fig. 4. Logical diagram of the system running control (a) solar system; (b) ASHP unit; (c) heat supply.

(totally 480 h). Temperatures of Rooms 5 and 6 are obviously lower than Rooms 1–4 because there is no heat supply to Rooms 5 and 6. Fig. 9 shows the comparison of the simulated Room 1 temperature with the measured values during the test period. The whole trend is close, although there are local deviations between each other. The error might be attributed to several reasons: the simulation was based on the multi-zone building model of the lumped

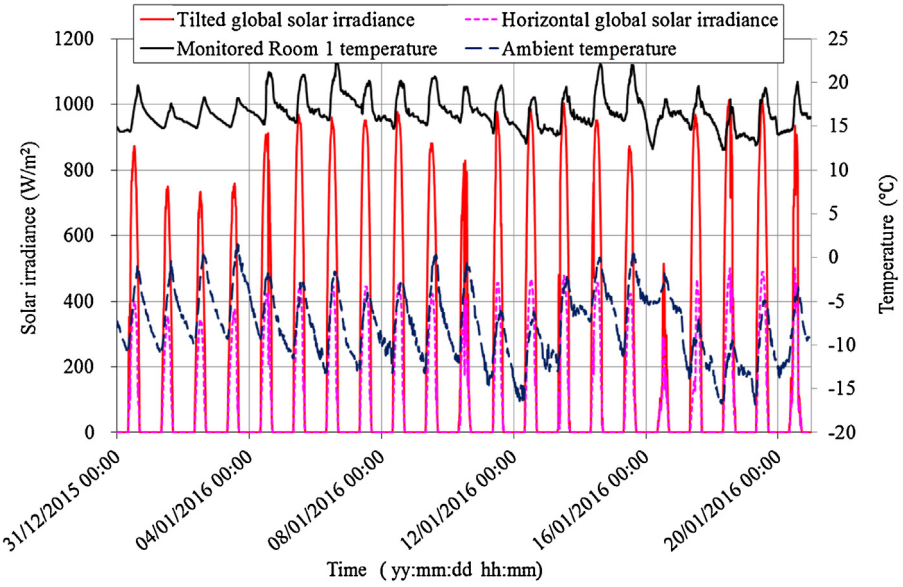

Fig. 5. Measured meteorological conditions and indoor temperature of Room 1.

Table 1
Measuring instruments for the tests.

Names of instruments	Measurement range	Accuracy	Function
Temperature automatic recorder (WZY-1)	−40–100 °C	±0.3 °C	Measure the indoor and outdoor temperatures
Thermocouple (T type)	−50–300 °C	±0.5 °C	Measure the tank temperature, inlet and outlet temperatures for the solar system and the main pipes of the heat supply
Turbine flowmeter (LW-25D2ASDS)	0–1.5 m^3/h	±1.0%	Measure the volume flow rates respectively for the solar system, the condenser side of the ASHP and the main pipes of the heat supply
Ultrasonic combined heat meter	0–9999 MWh	±2.0%	Measure the accumulated heat quantities for each sub-systems
Electricity meter	0–99999 kWh	±1.0%	Measure the electricity consumption of the ASHP
Pyranometer (TBQ-2)	0–2000 W/m^2	±2.0%	Measure the inclined and horizontal global solar irradiances

thermal capacitance method which does not precisely characterize the dynamic thermal characteristics of the building envelopes; the room air exchange rate was selected as 0.5 h^{-1} as per rule of thumb, and so on. The real room air exchange rate is variable due to occupants' behavior [12] and unsteady flow state. Fig. 10 makes the comparison of the simulated hot water supply temperature with the measured values during the test period.

Table 5 lists the comparison of the simulation results with the field test data of the space heating system thermal performance. The parameters accumulated heat supply, heat energy collected by the solar system, heat energy provided by the ASHP, average solar thermal efficiency, solar fraction (contribution ratio) and the average heat load index during the 20 days' test period are considered. It is found that, the relative errors of the accumulated heat energy and the solar fraction are within 5%, while that of the average heat

Table 2
Thermophysical property parameters of the building envelope of the pilot rural house.

Component	Material	Thickness (mm)	Thermal conductivity, W/(m K)
External wall (except south wall)	Lime mortar (inner)	20	0.93
	Common brick masonry	370	0.81
	EPS insulation	60	0.04
	Lime mortar (outer)	20	0.93
South wall	Lime mortar (inner)	20	0.93
	Common brick masonry	370	0.81
	Lime mortar (outer)	20	0.93
Interior wall	Lime mortar	15	0.93
	Common brick masonry	120	0.81
	Lime mortar	15	0.93
Roof	Tile	50	1.50
	Mineral wool	5	0.05
	Spruce pin	50	0.13
	Air layer	800	0.03
	Plaster card	20	0.23

Table 3
Comprehensive heat transfer coefficients (U-values) of the building envelopes.

Types of the building envelope surfaces	Structure and size	Comprehensive heat transfer coefficient, W/(m^2 K)
External wall (except south wall)	20 mm lime mortar (inner) + 370 mm common brick masonry + 60 mm EPS insulation + 20 mm lime mortar (outer)	0.460
South wall	20 mm lime mortar + 370 mm common brick masonry + 20 mm lime mortar	1.486
Interior wall	15 mm lime mortar + 120 mm common brick masonry +15 mm lime mortar	2.836
Roof	50 mm tile + 100 mm wood + 30 mm suspended ceiling	1.069
Ground floor	100 mm concrete slab	0.039
Window	Double-layer plastic steel window	2.9
Door	Double-layer plastic steel material	2.9

Note: The indoor and outdoor convective heat transfer coefficients h_{in}, h_{out} for the vertical surface in Beijing are 3.5 W/(m^2 K) and 23.3 W/(m^2 K), respectively, provided in DesT manual [11].

Table 4
Main TRNSYS components and parameter settings (default condition).

Name	Component type	Main parameters	Descriptions
Building	Type 56	Room air exchange rate: 0.5 h$^{-1;}$ Heating type: the default room controlled temperature is 18 °C and heating powers of Rooms 1–4 correspond to the radiators' heat transfer rates	Multi-zone building model; For the thermophysical properties please see Table 2;
Rad_Rooms 1–4	Type 1231	Design capacity: 1.9 kW; Design surface temperature: 55 °C; Design delta_T exponent: 1.3; Number of pipes: 18 (Diameter: 32 mm)	Terminal radiators used for Rooms 1–4
Space Heating	Type 108	1st stage heating setpoint: 18 °C; Temperature dead band: 2 °C; Monitoring temperature: Room 1	The logical control is described in Fig. 4(c)
HP-ET-Collector	Type 438	Series collector gross area: 18.8 m^2; Collector capacitance: 470 kJ/K; Tested flow rate: 0.02 kg/(s m^2); Zero loss efficiency: 0.479; Tested 1st order loss coefficient: 1.437 W/(m^2 K); Tested 2st order loss coefficient: 0.001 W/(m^2 K^2)	The thermal performance parameters obtained from the manufacture
Tank	Type 4a	Tank volume: 0.3 m^3; Tank heat loss coefficient: 0.833 W/(m^2 K); 3 nodes for the storage tank with 0.5 m height for each node	The tank was not well structured for thermal stratification thus 3 nodes were chosen
Pump 1–3	Type 3	Flow rates of the solar system, the ASHP condenser side and the heat supply were 0.6, 0.9, 0.8 m^3/h, respectively; The flow rate into the radiators were assumed to be uniform using Type 647 (Diverting-2)	The pump start and stop signals were logically calculated by equations according to Fig. 4.
ASHP	Type 1247	Rated heating capacity: 8 kW; Rated heating power: 2.25 kW; Rated air flow rate: 1080 m^3/h; Rated liquid flow rate: 1.01 m^3/h	The type component uses normalized performance data and correction factor data which suit for general cases
Weather_data1	Type 15	Input Beijing typical meteorological year data	Used for the optimization analysis
Test conditions	Type 99	Input the measured meteorological conditions during the test	Used for the model validation.
T&Loadprint	Type 25c	Using equations and Type 24 as the input parameters	Printed the calculating results

Table 5
Comparison of the simulation results and the field test data of the system thermal performance.

Parameters	Test results	Simulation results	Relative error compared to the test
20 days' accumulated heat supply (GJ)	2.82 × 3.6 = 10.152	10.045	−1.1%
20 days' accumulated heat energy collected by solar system (GJ)	0.59 × 3.6 = 2.124	2.233	5.1%
20 days' accumulated heat energy provided by the ASHP (GJ)	2.23 × 3.6 = 8.028	8.145	1.5%
Average solar thermal efficiency based on the gross area (−)	31.3%	36.2%	15.7%
Solar fraction f (−)	20.9%	21.5%	2.9%
Average heat load index (W/m^2)	68.7	74.3	8.2%

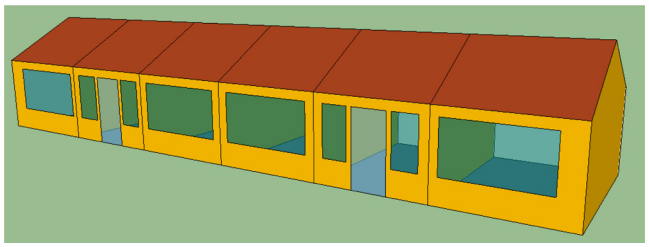

Fig. 6. Building geometrical model of the pilot rural house based on Google Sketchup embedded Trnsys 3d plug-in.

load index is 8.2%. The relative error of the average solar thermal efficiency is 15.7%. The simulation results show that the calculation error could be accepted in real engineering, which suggests the simulated model is reasonable for the following analysis.

4. Optimization analysis of the solar space heating system for a typical single family rural house in Beijing

The techno-economic influence factors of the solar space heating system for a single family house are complicated. The design layout and building envelope materials of the house, the occupants' behaviours and room air exchange rate, the system matching

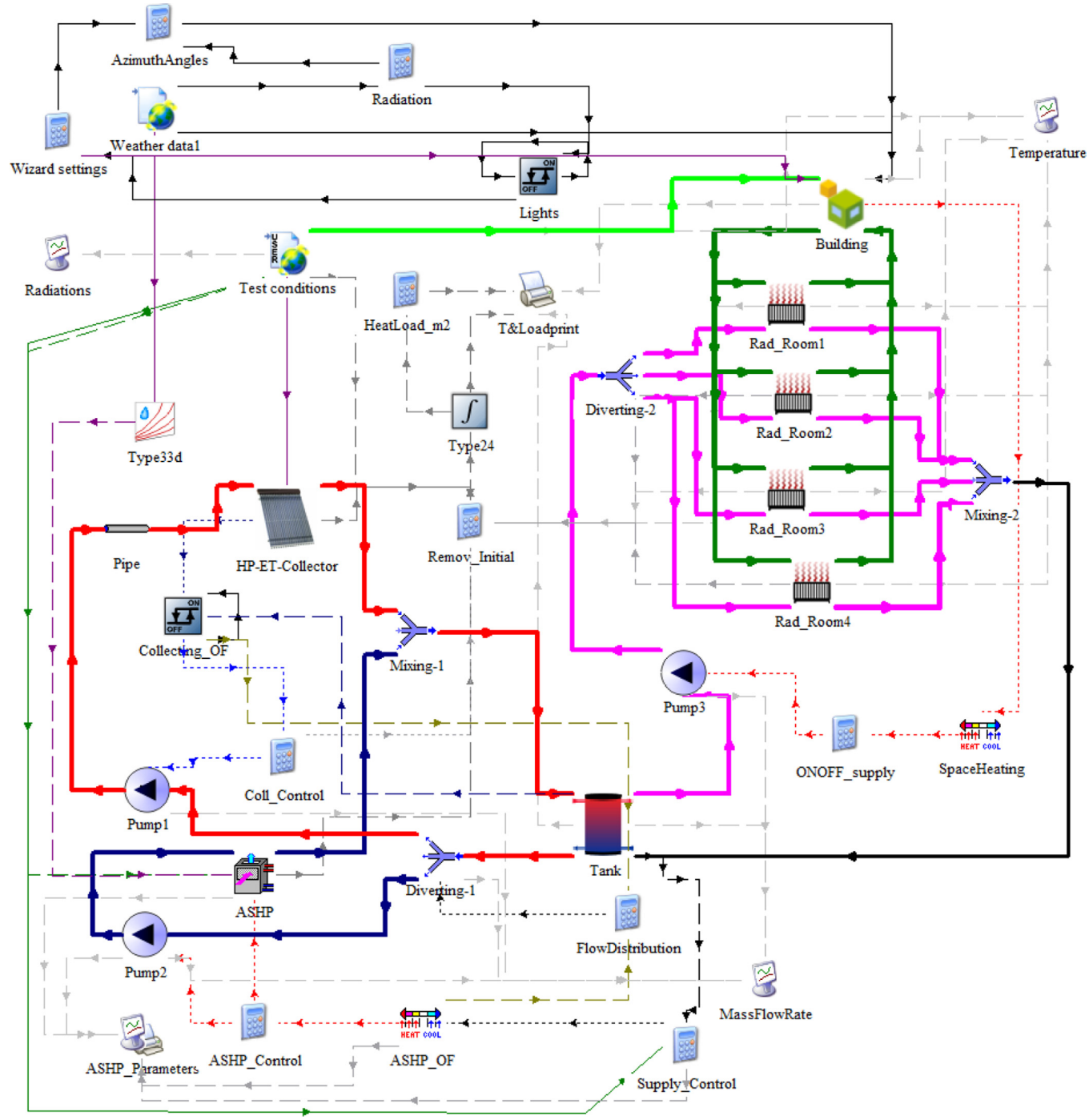

Fig. 7. TRNSYS based system quasi-dynamic thermal performance simulation model coupled with the multi-zone building model (TYPE 56) for the integrated space heating system.

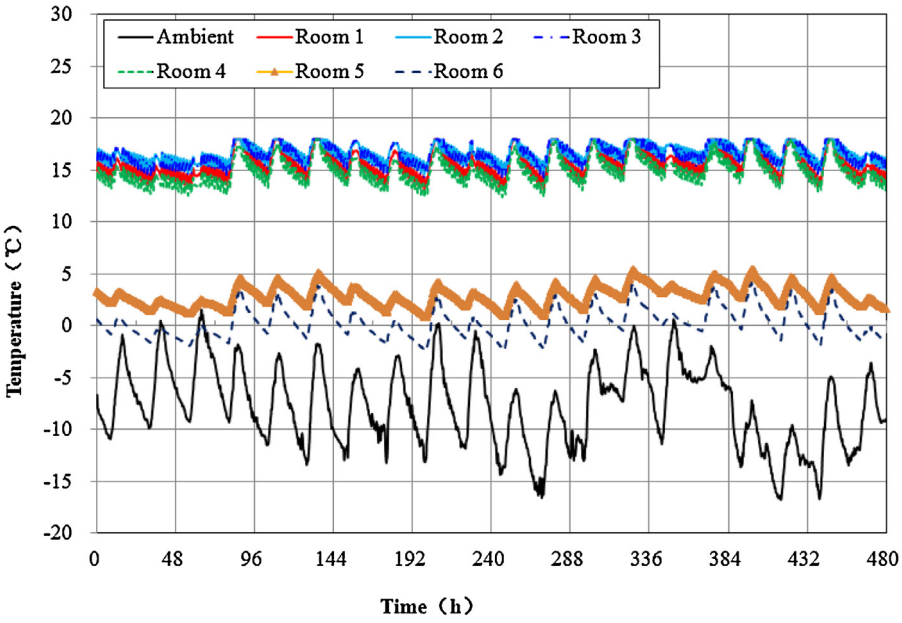

Fig. 8. Simulated temperatures of Rooms 1–6 during the 20 days test period.

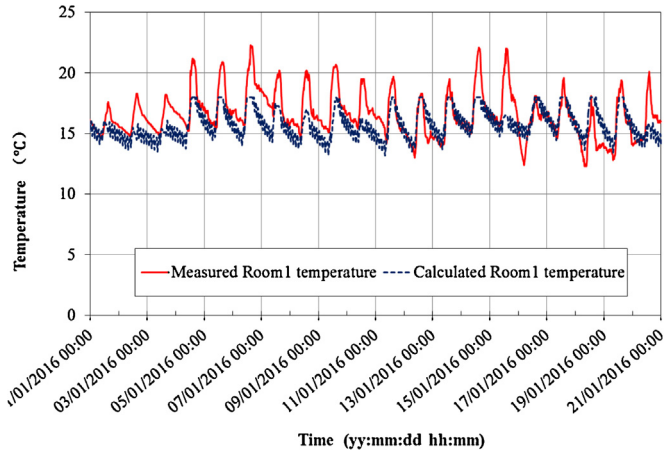

Fig. 9. Comparison of the simulated Room 1 temperature with the measured values during the test period.

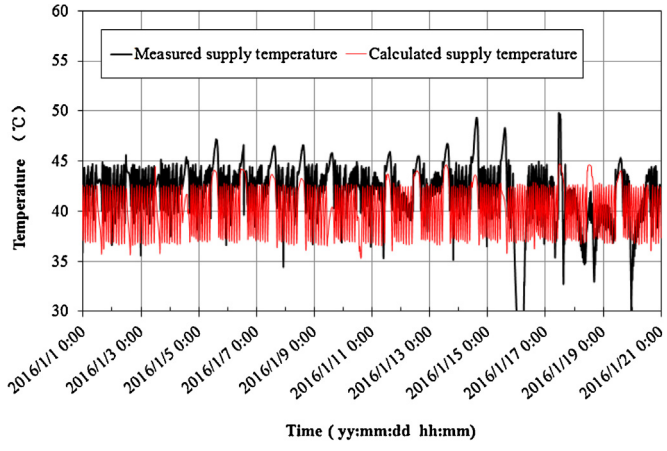

Fig. 10. Comparison of the simulated hot water supply temperature with the measured values during the test period.

design and control strategies, etc. could affect the economical efficiency of the solar heating system to different extents. To find the primary influence parameters it is therefore needed to firstly optimize the solar heating system of the established pilot engineering. The effect of the building thermophysical property will be considered secondly.

4.1. Parameter sensitivity analysis of the existing pilot system

4.1.1. The benchmark condition

The model input parameters of the benchmark (default) condition can be found in Table 4. For the system optimization, the typical meteorological year's data is adopted to simulate the building space heating thermal performance of the rural house. The winter space heating period of Beijing is 121 days starting from November 15th to March 15th of the next year, corresponding to the hour numbers of 0–1776 h and 7632–8760 h in the whole year. For the simulation of the established pilot system in winter period on the benchmark condition, the accumulated heat supply, the solar collecting heat energy, the heat energy provided by the ASHP are 54.7 GJ, 10.6 GJ, 44.1 GJ, respectively. The calculated average heat load index during winter is 64.9 W/m^2, while the average winter temperature of the Room 1 is 17.8 °C, which is slightly lower than the target temperature 18 °C. Besides, during winter the average solar thermal efficiency is 43.7% and the solar fraction is 19.4%. It suggests that 80.6% heat is supplied by the ASHP with the present running parameters.

4.1.2. The minimum tank target temperature for different room target temperature conditions

In order to find the minimum tank target temperature (also the heat supply temperature) for the established pilot system, different tank target temperature conditions were calculated with the Room 1 target temperature at 18 °C, as shown in Fig. 11. It is found that the minimum tank target temperature (the condition of which is encircled by an ellipse) for Room 1 temperature at 18 °C is 46 °C, with a winter average heat load index of 68.7 W/m^2 and a solar fraction of 18.2%.

For different conditions of Room 1 target temperatures such as 16 °C, 18 °C, 20 °C, the minimum tank target temperatures are 43 °C, 46 °C, 52 °C, respectively. The corresponding average winter heat

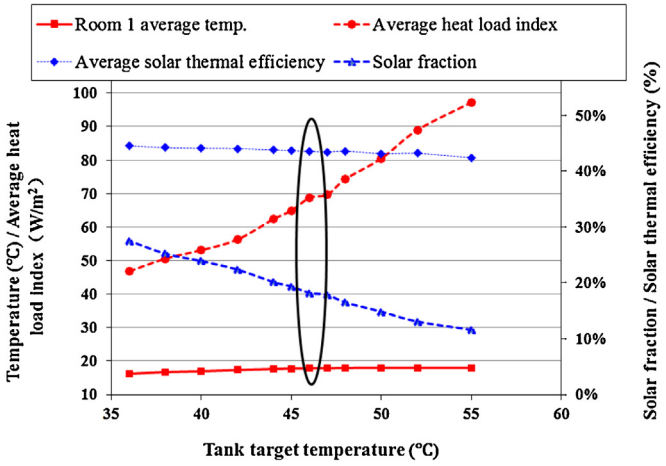

Fig. 11. Simulated system parameters for different target tank temperature conditions with the target Room 1 temperature at 18 °C.

load indices are 61.9 W/m^2, 68.7 W/m^2, 82.6 W/m^2, which means that the minimum energy consumptions of Room 1 target temperature at 18 °C, 20 °C are increased by 11.0%, 33.4% compared to that of 16 °C, respectively. Additionally, the solar fraction for Room 1 target temperature at 18 °C, 20 °C are decreased by 9.5%, 27.4%, respectively.

4.1.3. Running mode of the solar collecting system

The solar collecting circulation for the established system adopted temperature difference control to start and stop the circulating pump, as illustrated by Fig. 4(a). Fig. 12 considers the running mode of the solar system controlled by fixed collector outlet temperture, in order to determine which of the two control modes is better. In the control mode by fixed collector outlet temperture, the pump flow rate is changeable by using the PID controller (Type 23) to obtain a relatively constant outlet temperature (e.g. 60 °C). The start and stop of the pump is controlled by setting an effective critical global solar irradiance 400 W/m^2 according to real engineering experience.The calculated solar thermal efficiencies for different conditions of fixed collector outlet tempertures 60 °C, 65 °C, 70 °C are nearly the same, with a value of 40%, which is 8.3% lower than the control mode by temperature difference under the condition of the Room 1 target temperature at 18 °C and heat supply temperature at 46 °C. The solar fraction of the three fixed collector outlet temperture conditions is evenly decreased by 11.5% compared to the condition of temperature difference control. It suggests the control mode of the solar system by temperature difference is superior to that by fixed collector outlet temperature.

4.1.4. Different tank volumes

The conditions of different tank volumes were also considered to compare the differences. Fig. 13 gives the calculated system parameters for different tank volumes with the Room 1 and tank target temperatures at 18 °C, 46 °C, respectively. It is found that there is a minimum suitable tank volume (300 L) for the established pilot system, the condition of which is enclosed by an ellipse in Fig. 13. In the cases of tank volumes 200 L and 250 L, the average heat load indices are lower than the other calculated cases but the Room 1 temperatures are also lower than 18 °C (target temperature). Because too small tank volume results in frequently start and stop of the ASHP, the time period of room temperature deviating from the desired room temperature is longer than the case of a suitable tank volume, directly resulting in a lower Room 1 average temperature. Hence, the minimum suitable tank volume should be chosen for a solar system.

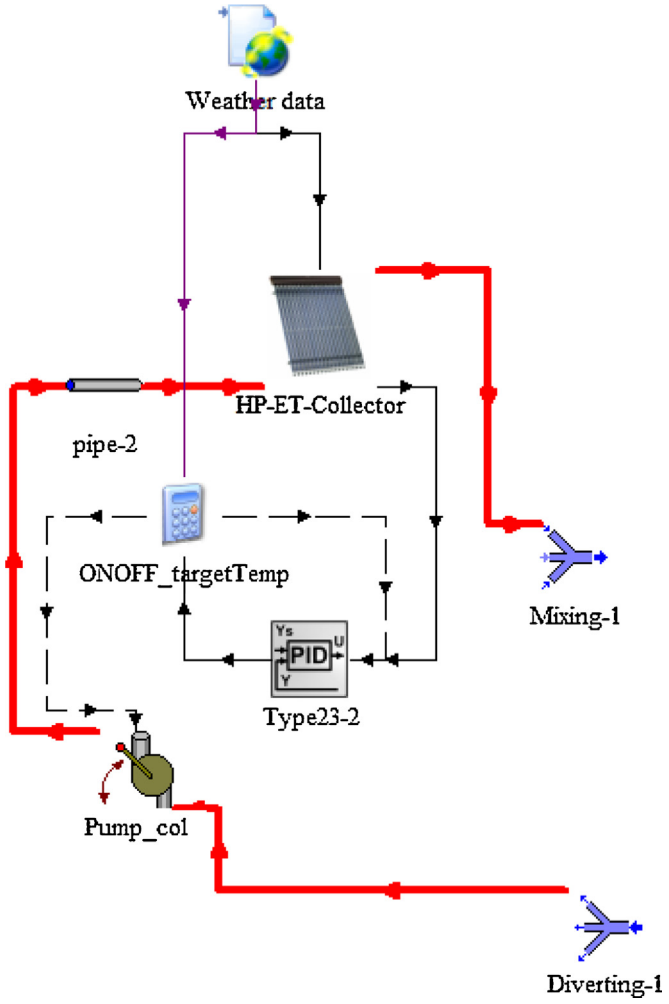

Fig. 12. Logical control mode of fixed collector outlet temperture.

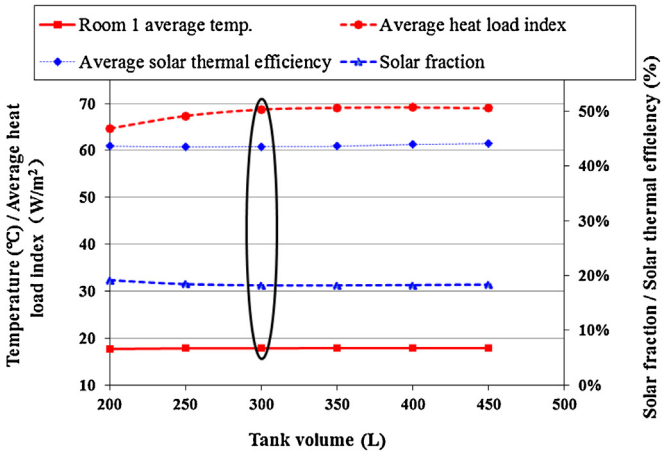

Fig. 13. Simulated system parameters for different tank volumes with the Room 1, tank targets temperatures at 18 °C, 46 °C, respectively.

4.2. System optimization for a typical single family rural house with good building insulation

In the previous sensitivity analysis, the winter heat load index of the pilot rural house is high. The condition of minimum tank target temperature at 46 °C for Room 1 temperature at 18 °C has an average winter heat load index of 68.7 W/m^2 and the solar fraction

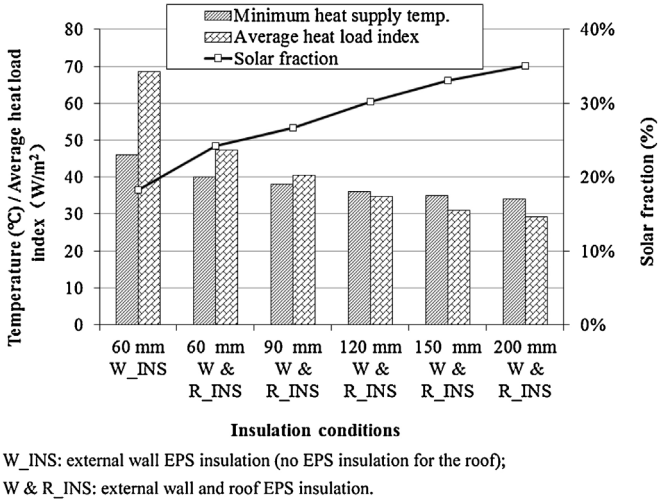

Fig. 14. Parameters for different thermal insulation conditions.

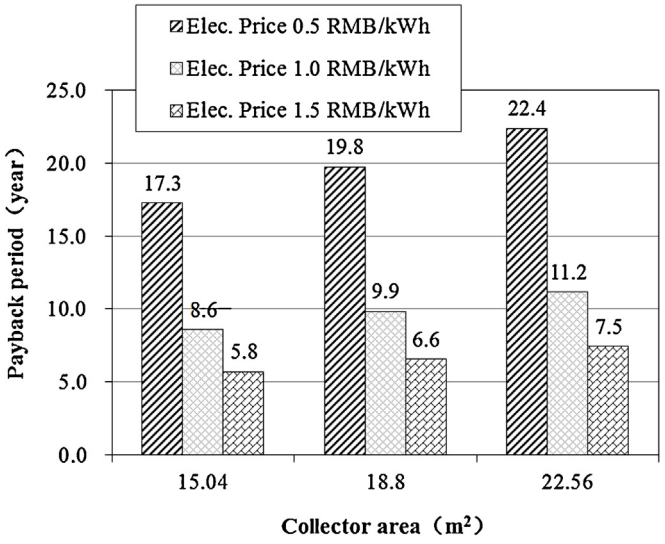

Fig. 15. Payback period of the integrated system compared to the condition of fully ASHP space heating for the pilot household (60 mm ESP insulation for external wall).

of the system is just 18.2%. It is presumed that higher solar fraction may improve the system economical efficiency. To improve the solar fraction from the view point of building energy conservation [13], increasing insulation of the building envelope is considered to reduce the winter heat load.

Conditions of different EPS insulation thicknesses 60 mm, 90 mm, 120 mm, 150 mm, 200 mm were simulated. Fig. 14 shows the calculated minimum heat supply temperatures, average winter heat load indices and solar fractions in different EPS insulation conditions with the Room 1 target temperature at 18 °C. It is found that increasing 60 mm EPS insulation for the roof can decrease 31% winter heat load. And the heat load index gradually decreases while solar fraction increases with insulation thickness increasing. When the insulation thickness is larger than 120 mm, the decreasing extent of the winter heat load is not significant. For the case of 120 mm EPS insulation, the average heat load index is 34.8 W/m^2, which is nearly half of the benchmark condition. The solar fraction can increase from previously 18.2% to 30.2%. So it is reckoned to be good insulation for the system economic analysis.

4.3. Economic analysis of the solar space heating system combined with the ASHP

Different solar collector areas are considered to undertake the economic analysis of the solar space heating system. Since the roof of a typical rural house usually has an area of about 25 m^2 for collector installation, three conditions of solar collector areas 15.04 m^2, 18.80 m^2, 22.56 m^2 are chosen, corresponding to 4, 5, 6 collector modules (3.76 m^2 for each in gross area), respectively. The solar fraction of the three cases are respectively 26.1%, 30.2%, 33.9% with the minimum tank target temperature at 36 °C and the Room 1 target temperature at 18 °C. The solar heating systems with different collector areas combined with the ASHP are compared with the reference condition of the fully ASHP space heating. The initial cost of the solar system can be paid back by annually saving running electricity cost compared with the reference condition. Assuming the electricity price per kWh (C_{elec_price}) is a constant in the whole system life span, the annual payback cost ($\Delta C_{payback,ann}$) can be calculated by the running electricity cost of the reference condition subtracting the electricity costs of the integrated heating system, as given by Eq. (5).

$$\Delta C_{payback,ann} = C_{ASHP\_sig,ann} - C_{ASHP\_comb,ann} - C_{sol\_pump,ann} \quad (5)$$

where the annual running electricity cost ($C_{ASHP\_sig,ann}$) of the reference condition, the integrated system by the ASHP ($C_{ASHP\_comb,ann}$) and that by the solar circulating pump ($C_{sol\_pump,ann}$) are calculated by Eqs. (6)–(8), respectively.

$$C_{ASHP\_sig,ann} = P_{e,ASHP} \times C_{elec_price} \quad (6)$$

$$C_{ASHP\_comb,ann} = P_{e,ASHPcomb} \times C_{elec_price} \quad (7)$$

$$C_{sol\_pump,ann} = P_{sol\_pump} \times H_{sol\_pump} \times C_{elec_price} \quad (8)$$

In which, $P_{e,ASHP}$ is the total electricity consumption of the reference condition during winter space heating period, kWh; $P_{e,ASHPcomb}$ is the total electricity consumption by the ASHP in the integrated heating system during winter, kWh; P_{sol_pump} is the input electric power of the solar circulating pump, 0.18 kW in the present study; H_{sol_pump} is the annual running hours of the solar circulating pump during winter, h; the units of all the costs are in RMB.

According to the life cycle cost assessment [8] regardless of the inflation and discount rate, the static payback period n (years) of the solar space heating system compared with the fully ASHP space heating is calculated by

$$n = C_{sol,init\_invest} / \Delta C_{payback,ann} \quad (9)$$

where $C_{sol,init\_invest}$ is the total initial cost of the solar system, RMB. In the present study, the total construction cost of the solar system with 18.8 m^2 collector area is 30,000 RMB. Thus a uniform unit cost of 1600 RMB/m^2 collector for the three collector area conditions is presumed to further analysis since the scales of the different collector areas are close to each other.

Figs. 15 and 16 give the payback periods of the solar space heating system for the established pilot household as well as the cases with 120 mm EPS insulation of the building envelope, respectively, assuming three levels of electricity price at 0.5, 1.0, 1.5 RMB/kWh. It is found that the payback period becomes longer as the collector area increases at a fixed electricity price. For a lower electricity price, the increasing extent of the payback period as collector area is less significant compared to a higher electricity price. For the pilot household with 60 mm exterior wall insulation of the building envelope, the payback periods of the solar systems are economical when the electricity price is 1.5 RMB/kWh. However, the current electricity price is around 0.5 RMB/kWh in the rural region of Beijing, which means a long payback period of 17.3–22.4 years.

Moreover, the payback periods for the cases of a typical rural house with good insulation in Fig. 16 are longer than the corresponding cases with the existing insulation. Good building insulation only helps to improve the solar fraction during the winter

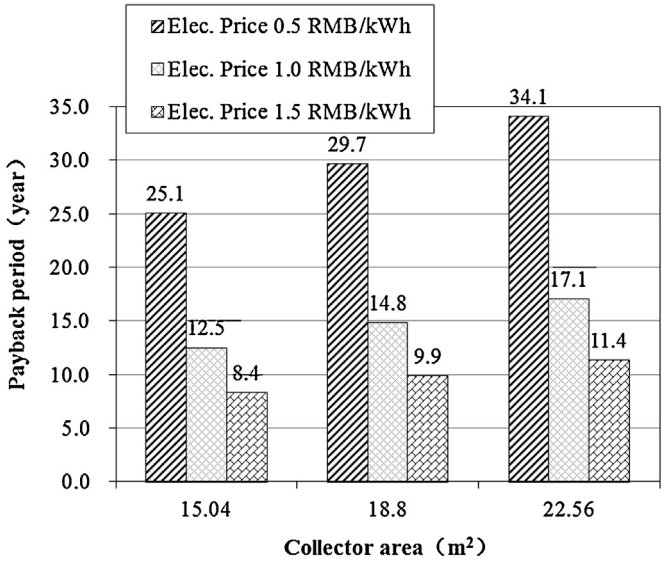

Fig. 16. Payback period of the integrated system compared to the condition of fully ASHP space heating with 120 mm EPS insulation of the building envelope.

heating period. It is further found that, the payback period mainly depends on the equivalent solar heat price per kWh ($C_{eq,heat\_price}$) simply calculated by Eq. (10), but has little relationship with the building insulation.

$$C_{eq,heat\_price} = \frac{C_{sol,init\_invest}}{N \cdot Q_{ann,solarheat}} \quad (10)$$

where $C_{sol,init\_invest}$ is the initial cost of the solar system, RMB; N is the system life span, 25 years for the established solar system; $Q_{ann,solarheat}$ is the annual heat energy collected by the solar system, kWh. Take the case of 18.8 m^2 collector area for the pilot household as an example, the equivalent heat price per kWh is 0.41 RMB/kWh (=30 000 RMB/(25 year × 2920 kWh/year)).

The equivalent heat prices per kWh ($C_{eq,heat\_price}$) of the solar systems with collector areas 15.04 m^2, 18.80 m^2, 22.56 m^2 for the pilot household are 0.41, 0.41, 0.42 RMB/kWh, while those for the typical rural house with 120 mm EPS insulation of the building envelope are 0.43, 0.45, 0.46 RMB/kWh, respectively. Because the equivalent solar heat prices are very close to the electricity price level of 0.5 RMB/kWh, the cost difference between the average annual cost of the solar system and the annual running cost of the ASHP is small, directly resulting in a long payback period. In order to improve economical efficiency of the solar system, it is needed to reduce the equivalent solar heat price per kWh, which can be realized by cutting down the cost of the solar system per m^2 collector area and improving the accumulated solar thermal energy (e.g., improving the solar thermal efficiency, installing collectors in good solar radiation regions, etc.) according to Eq. (10). Hence, the initial cost of the solar space heating system for the single family rural house are too high compared with the conventional energy source ASHP. To put forward the integrated solar space heating for reducing carbon emission under the current solar market cost price and collector technology, it is suggested the Beijing municipal government should offer some financial subsidy to reduce the equivalent solar heat price per kWh.

Besides, it is worth mentioning that the application of the integrated solar space heating can help to reduce carbon emission, although there is no carbon trade tax in the current China solar market. It is anticipated that in the soon future the carbon reduction effect of solar energy utilization will be put into effect, which will contribute to the system economical efficiency. The heat gain of 1 m^2 collector gross area is about 0.5–0.57 GJ/year in the present study. Since the carbon emission effect of the coal equivalent is 2.77 kg CO_2/kg coal and 1 tce (ton coal equivalent) corresponds to 29.3 GJ heat, the carbon emission reduction effect of the integrated solar space heating system employed is 47.3–53.5 kg CO_2/year per m^2 collector gross area.

5. Conclusions

Based on the thermal performance simulation model of a solar space heating system combined with an ASHP using TRNSYS 17.2 for the typical rural residential house, the system optimization design and economical efficiency were analyzed regarding both the existing pilot household and the typical rural house with good building insulation. It can be arrived at the following conclusions:

(1) There is a minimum heat supply temperature to satisfy the heat demand of the desired room target temperature. The control mode of the solar circulating system by temperature difference is superior to that by fixed collector outlet temperature. Besides, minimum suitable tank volume should be designed for the solar heating system. Regarding the established pilot system the minimum suitable tank volume is 300 L.
(2) The payback periods of the solar space heating system with the collector areas 15.04–22.56 m^2 are 17.3–22.4 years for the studied pilot household with the electricity price at 0.5 RMB/kWh (which is adjacent to the current electricity price in the rural region of Beijing). The payback period of the solar system for the typical rural house with good building insulation is longer than that of the studied pilot household, although good building insulation improves the solar fraction of winter space heating.
(3) It is found that the payback period of the solar space heating system is closely related to the equivalent heat price per kWh of the solar system. The equivalent heat prices for the established pilot household and the rural house with 120 mm EPS insulation are about 0.41–0.42 RMB/kWh, 0.43–0.46 RMB/kWh, respectively. They are too high for system application. The equivalent heat price can be reduced by cutting down the cost of the solar system per m^2 collector area and improving the accumulated solar thermal energy (e.g., improving the solar thermal efficiency or installing the solar system in good solar radiation regions). To put forward the integrated solar space heating in single family rural houses for reducing carbon emission under the current solar market cost price and collector technology, it is suggested that the Beijing municipal government should offer some financial subsidy to compensate the equivalent solar heat price per kWh. Besides, the carbon emission reduction effect of the integrated solar space heating system employed is 47.3–53.5 kg CO_2/year per m^2 collector gross area.

Acknowledgment

This work was supported by the National Natural Science Foundation of China (Grant No. 51506193), China Scholarship Council (CSC No. 201504910177), Beijing Municipal Science and Technology Project (No. 141100002714001) and Guangdong Innovative and Entrepreneurial Research Team Program (No. 2013N070). The authors thank to the engineer Qiang Zhang and their colleagues in Beijing Tsinghua Solar Science and Technology Co., Ltd. for the pilot system construction and establishment.

References

[1] M. Evans, S. Yu, B. Song, Q. Deng, J. Liu, A. Delgado, Building energy efficiency in rural China, Energy Policy 64 (2014) 243–251.

[2] R. Zhang, J. Jing, J. Tao, S.-C. Hsu, G. Wang, J. Cao, C.S.L. Lee, L. Zhu, Z. Chen, Y. Zhao, Z. Shen, Chemical characterization and source apportionment of PM2. 5 in Beijing: seasonal perspective, Atmos. Chem. Phys. 13 (2013) 7053–7074.
[3] S. Lu, W. Feng, X. Kong, Y. Wu, Analysis and case studies of residential heat metering and energy-efficiency retrofits in China's northern heating region, Renew. Sustain. Energy Rev. 38 (2014) 765–774.
[4] M. Shan, T. Yu, X. Yang, Assessment of an integrated active solar and air-source heat pump water heating system operated within a passive house in a cold climate zone, Renew. Energy 87 (2016) 1059–1066.
[5] J. Li, X. Li, N. Wang, Y. Hu, R. Feng, Experimental research on indoor thermal environment of new rural residence with active solar water heating system and external wall insulation, Appl. Therm. Eng. 95 (2016) 35–41.
[6] A. Arsalis, A.N. Alexandrou, Parametric study and cost analysis of a solar-heating-and-cooling system for detached single-family households in hot climates, Sol. Energy 117 (2015) 59–73.
[7] Y. Hang, M. Qu, F. Zhao, Economic and environmental life cycle analysis of solar hot water systems in the United States, Energy Build. 45 (2012) 181–188.
[8] B. Huang, V. Mauerhofer, Life cycle sustainability assessment of ground source heat pump in Shanghai, China, J. Clean. Prod. 119 (2016) 207–214.
[9] X. Li, M. Gul, T. Sharmin, I. Nikolaidis, M. Al-Hussein, A framework to monitor the integrated multi-source space heating systems to improve the design of the control system, Energy Build. 72 (2014) 398–410.
[10] TRNSYS, A Transient Simulation Program, Version 17, University of Wisconsin Solar Energy Laboratory, Madison, WI, 2012.
[11] D. Yan, J. Xia, W. Tang, F. Song, X. Zhang, Y. Jiang, DeST – an integrated building simulation toolkit part I: Fundamentals, Build. Simul. 1 (2008) 95–110.
[12] S. Wei, R. Jones, P.D. Wilde, Driving factors for occupant-controlled space heating in residential buildings, Energy Build. 70 (2014) 36–44.
[13] M. Shan, P. Wang, J. Li, G. Yue, X. Yang, Energy and environment in Chinese rural buildings: situations, challenges, and intervention strategies, Build. Environ. 91 (2015) 271–282.